PHYSICAL REVIEW B VOLUME 26, NUMBER 10 15 NOVEMBER 1982

Impurity states in doped *trans*-polyacetylene

Garnett W. Bryant
Surface Science Division, National Bureau of Standards, Washington, D.C. 20234

Arnold J. Glick
Department of Electronics, Weizmann Institute of Science, Rehovoth, Israel
*and Department of Physics, University of Maryland, College Park, Maryland 20742**

(Received 1 July 1982)

We assess the importance of the impurity states of a doped *trans*-polyacetylene chain. The impurity potential is modeled by a point charge that is located off the chain and is screened phenomenologically. The common assumption that the dopant levels of a dimerized chain closely approximate the hydrogenic levels of a point charge is invalid if the impurity is not on the chain, even if the dopant is screened by the bulk dielectric constant. Additional nonhydrogenic states occur well into the gap. The formation energies for charged kink and polaron lattice distortions are found by solving the Su-Schrieffer-Heeger model for polyacetylene with an impurity added. The impurity states severely alter the structure and states of kink and polaron distortions. Moreover, the modifications depend sensitively on the form of the dopant potential. For the dopant screened isotropically by the bulk dielectric constant, the kink distortion has gap states inconsistent with the observed midgap optical absorption. In contrast, the polaron distortion is both stable and predicts a consistent optical threshold. The nature of doping polyacetylene will remain unclear until a realistic model for the dopant and its interaction with polyacetylene has been developed.

I. INTRODUCTION

Considerable excitement has been stirred by the suggestion of Su, Schrieffer, and Heeger[1,2] (SSH) and of Rice[3] that kinklike (or equivalently, solitonlike) lattice distortions exist in lightly doped *trans*-polyacetylene, $(CH)_x$, and that these excitations strongly affect the magnetic and optical properties of the system. They argue that the charge transfer from the dopant to the $(CH)_x$ chain occurs via kink formation because less energy is needed to create a neutral kink on the polymer chain and occupy its midgap state with the transferred charge than is required to transfer the charge to an impurity state of the chain. Implicit in this argument is the assumption that the dopant potential is weak, so that the energy bands are nearly rigid, the impurity states are near the band edges, and these states do not contribute to the midgap optical absorption or modify the kink distortions. The observation of midgap absorption in doped $(CH)_x$ by Suzuki *et al.*[4] and by Kiess *et al.*[5] supports the kink mechanism for doping.

Unfortunately, the intuitively appealing arguments[6] used to show that the dopant potential has little effect on the chain or any kink distortions of the chain are incorrect when applied to one-dimensional systems such as $(CH)_x$, as we have pointed out in a recent paper.[7] Even weak dopant potentials can modify the energy bands. The shifts induced by the dopant can be larger than those shifts caused by lattice distortions. Consequently, dopants also alter the states, shapes, and energies of the lattice distortions. In this paper we elaborate on Ref. 7, providing detailed results not originally discussed and extending our investigations to cover model dopant potentials not considered before.

No accurate model has been developed for the impurity potential in lightly doped $(CH)_x$. Instead, the assumptions are usually made that complete charge transfer occurs and that the dopant can be considered as a point charge located off the chain.[2,6,8] Furthermore, the point charge is screened phenomenologically with an isotropic bulk dielectric constant ($\epsilon \simeq 10$). The actual screening may not be complete near the impurity. If incomplete screening is included, then the potential is stronger than the fully screened potential. In addition, $(CH)_x$ is anisotropic. The dielectric response parallel to the chains is much greater than the response perpendicular to the chains. The resulting anisotropic screening is ignored if an isotropic bulk dielectric constant is used.

Because there are no good *a priori* models for the

dopant and the screening, we limit our attention to phenomenological models for the interaction. These models are not meant to replace the more complete treatments of the impurity potential and screening that should be done. Rather, the models are used to show that kinks and polarons can be severely altered by the dopant, to illustrate the sensitivity of the results to the form of the dopant potential, to point out the wide range of results that occur for different potentials, and to motivate the need for fundamental treatments of the impurity potential. We focus on three aspects of modeling the interaction: (i) the position of the dopant relative to the chain—whether, for example, it is adjacent to a lattice site or to the middle of a bond, (ii) the local screening correction, and (iii) the anisotropic screening. We will consider the approximation that the dopant is a point charge in a future paper. Complex molecules such as I_3, AsF_5, and NH_3 are used as dopants. Karasz *et al.*[9] have suggested that the linear molecule I_3^+ lies parallel to the chain with half of a charge at each end of the molecule. Such "double-well" potentials should provide additional modifications to the electron states and the energies of lattice distortions.

We investigate the effect of the dopant on fully dimerized lattices, on lattices with kink distortions,[1–3] and on lattices with polaronlike distortions.[10] The kink is a domain wall which interpolates between the two degenerate ground states of $(CH)_x$. The polaron is a local relaxation of the fully dimerized bond alternation along the chain. The phase of bond alternation is the same on both sides of the polaron. Both distortions are described by specific functional forms for the shift of each lattice site and are parametrized by the halfwidth, the amplitude (for the polaron), and the position of the center of the distortion. In a general lattice distortion, the position of each site would be allowed to vary independently. We limit our attention to the polaron and kink distortions because they are the ones normally considered and because they are much simpler to study than those which are unrestricted. For a variety of model dopant potentials we determine the energies of kink and polaron distortions, the energies of gap states and impurity states associated with the distortions, and the densities of states.

Most significantly, we find that even a fully screened dopant modifies the states and energies of kinks and polarons. Both the charged pinned kink and charged pinned polaron are stable distortions, but only the charged polaron has gap states consistent with the observed midgap absorption. Moreover, for strong potentials with incomplete local screening the discrete nature of the $(CH)_x$ lattice is crucial. Pinned kinks with different bond configurations near such an impurity (the weak and strong kinks discussed later) are different. In addition, polarons centered on opposite sides of an impurity are different. Continuum models[11] for $(CH)_x$ will not be adequate in these situations.

In Sec. II we introduce the SSH Hamiltonian used to describe the π electrons of *trans*-$(CH)_x$. We also discuss the model dopant potentials and the different forms chosen for the screening. We also briefly discuss the intuitive arguments which asserted that impurity states were unimportant and we explain why they fail in one dimension. Finally we describe how the calculations were performed. In Sec. III we present the results obtained for kinks and polarons on doped and undoped chains and in Sec. IV we present our conclusions.

II. THE MODEL

We use the SSH model Hamiltonian to describe the π-electron system of $(CH)_x$,

$$H=\sum_{n,s} V_n(c^{\dagger}_{n+1,s}c_{n,s}+c^{\dagger}_{n,s}c_{n+1,s}) + \sum_n (K/2)(u_{n+1}-u_n)^2 . \quad (1)$$

$c^{\dagger}_{n,s}$ creates a π electron with spin s at CH group n, K is the spring constant for the σ-electron bond between adjacent CH groups, and u_n is the displacement of the nth group from its equilibrium position in a uniform lattice. The hopping integral that transfers π electrons between sites n and $n+1$ is

$$V_n=t_0+\alpha(u_{n+1}-u_n) .$$

A Peierls distortion occurs in the ground state. The lattice dimerizes with $u_n=(-1)^n u_0$ where u_0 is the amplitude of bond alternation (see Fig. 1). There are two degenerate ground-state configurations of dimerization, one obtained from the other by interchanging all the double and single bonds. In the dimerized lattice, two π-electron bands result with a gap between the conduction and valence bands. The density of states has square root singularities at the band edges.

We include the impurity potential by assuming[2,12] that the impurity produces an on-site energy shift at each site

$$U_{\text{imp}}=\sum_{n,s} U_n c^{\dagger}_{n,s}c_{n,s}-\sum_n U_n , \quad (2)$$

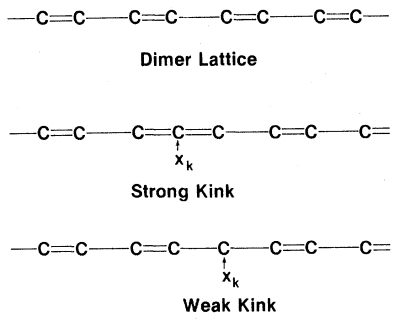

FIG. 1. Bond alternation patterns for a dimer lattice, a strong kink, and a weak kink. x_k denotes the kink center. C represents a CH group.

where U_n is the potential energy of an electron at site n due to the impurity. The interaction between the impurity and the charged $(CH)^+$ molecule at site n is assumed to be the same as that between an electron at site n and the impurity. It is the second term in Eq. (2). Including the lattice-impurity interaction does not qualitatively change the results.

We assume that the dopant is a point charge located a distance d from the chain[2,6,12] and that the screening of the dopant is described with a phenomenological dielectric function. The potential has the form (we assume that the impurity is a donor)

$$U_n=\frac{-e^2}{\epsilon(n)\,|\,(x_n-x_{\rm imp})^2+d^2\,|^{1/2}}\ . \tag{3}$$

where $x_n=na+u_n$ is the position of group n, a is the uniform bond length, and the impurity is a distance d from the chain, adjacent to the position $x_{\rm imp}$ on the chain. We assume that $x_{\rm imp}$ is either a lattice site or the middle of a particular bond (see Fig. 2). Normally the bulk static dielectric constant ($\epsilon\simeq 10$) is used[2,6,12] to screen the dopant. However,

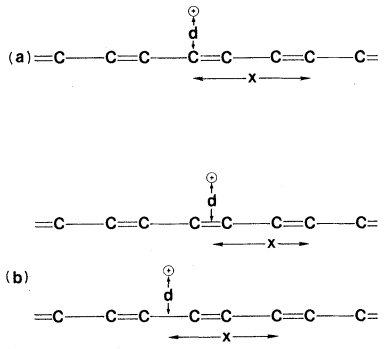

FIG. 2. Impurity configurations for (a) an impurity adjacent to a site and (b) impurities adjacent to weak and strong bonds. x is the distance along the chain relative to the impurity position.

this approximation ignores local corrections that should occur at sites near the impurity where the screening will be incomplete. We include these corrections by assuming that

$$\epsilon(n)=\epsilon_1+(\epsilon_2-\epsilon_1)\times\{1-\exp[-(\Lambda/a)\,|\,x_n-x_{\rm imp}\,|\,]\}\ . \tag{4}$$

ϵ_2 is the bulk dielectric constant and ϵ_1 is the constant near the impurity. Λ is the inverse decay length. The potential is a screened Coulomb potential at long range in this model.[13]

The screening in Eq. (3) is isotropic. However, $(CH)_x$ is anisotropic. Parallel to the chains $\epsilon_{||}\simeq 10$ while perpendicular to the chains $\epsilon_\perp\sim 1-3$. If a point charge is screened by such an anisotropic dielectric constant, as recently suggested by S. Kivelson (private communication), then

$$U_n=\frac{-e^2}{\epsilon_\perp\,|\,(x_n-x_{\rm imp})^2+\epsilon_{||}d^2/\epsilon_\perp\,|^{1/2}}\ . \tag{5}$$

Effectively, anisotropic screening moves the impurity farther from the chain by a factor $(\epsilon_{||}/\epsilon_\perp)^{1/2}$. However, the impurity is no longer screened by $\epsilon_{||}$ at large distances. Instead, the effective charge at long range is $e/\epsilon_\perp$. Both Eqs. (3) and (5) assume screening that is appropriate for a homogeneous system. This need not be the case on a microscopic scale for doped $(CH)_x$. However, as we have emphasized, these phenomenological models are used because they provide insight to the importance of the dopants and motivate the need for better models.

To explain why the dopant potential cannot be ignored, we consider a fully screened dopant ($\epsilon=10$ at each site). The potential is weak and the impurity states should be near the band edges. The $(CH)_x$ chain can be approximated by a one-dimensional linear chain and the effective-mass equation used to find the envelope function for the Wannier states. In the continuum limit,

$$\left[\frac{-\hbar^2}{2m_*}\frac{d^2}{dx^2}-\frac{e^2}{\epsilon\,|\,x^2+d^2\,|^{1/2}}\right]\psi(x)=E\psi(x)\ . \tag{6}$$

ψ is the envelope function, E the impurity level, m_* the effective mass, d the distance between the impurity and the chain, and x the distance along the chain (see Fig. 2). We use $d=2$ Å (Refs. 2 and 8) and $m_*=0.146m_e$. This effective mass can be obtained from the energy dispersion relations for the

conduction and valence bands as determined with the SSH model.

Fincher *et al.*[6] also assumed that d was small compared to the extent of the wavefunction and that $|x^2+d^2|^{1/2}$ could be replaced by $|x|$ in Eq. (6). This approximation reduces Eq. (6) to the one-dimensional Coulomb problem with the same energy levels as the three-dimensional problem. However, the approximation $d=0$ is invalid for any finite value of d and the lowest-energy level is much more bound than the hydrogenic level

$$E_0=-(e^2/2a_0)(m_*/m_e\epsilon^2) .$$

The approximation fails because there is a real, nonperturbative difference between the one-dimensional Coulomb problem and Eq. (6). The solutions to the one-dimensional Coulomb problem have the form[14,15]

$$\psi(x)=\begin{cases} xR(x), & x>0 \\ \pm|x|R(|x|), & x<0 . \end{cases}$$

The $R(x)$ are the radial wave functions of the three-dimensional problem. Even- and odd-parity wave functions both vanish linearly at the origin. The derivative of the even state is discontinuous at $x=0$ but this does not violate the wave equation because the potential is infinite at that point. Both the even and odd solutions have the same energy.

If the impurity is away from the chain, then the potential is finite everywhere. The odd-parity states still vanish at $x=0$ and their eigenvalues do not change much. However, the even solutions are finite at $x=0$. These states are less bound because the potential is weaker near $x=0$. The degenerate levels are split with even and odd states alternating in energy. For example, the lowest hydrogenic level, with degenerate even and odd states when $d=0$, splits into two states, an odd state with one node and an even state at higher energy with two nodes (see Fig. 3). In a similar manner, all bound states with a finite number of nodes are generated from the bound states obtained for $d=0$. However, the lowest eigenstate must be an even state with no nodes. This state cannot be obtained from the states found when $d=0$. To understand this, consider the argument in reverse. As d decreases, the potential becomes more attractive and the lowest state, with no nodes, becomes narrower. When d vanishes, this state approaches a δ function with an eigenvalue of $-\infty$. Such a state is unphysical and is not allowed when $d=0$. Physically, this extra even state does not occur if $d=0$ because the potential and, consequently, the kinetic energies are

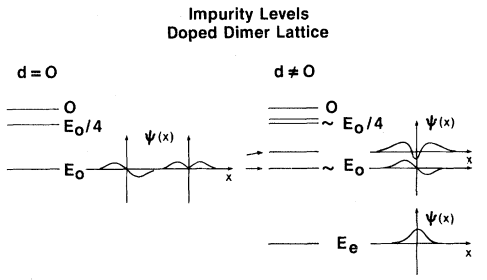

FIG. 3. Impurity levels and wave functions found with the effective-mass equation when the impurity is on the chain ($d=0$) and off the chain ($d\neq0$). Even and odd states are degenerate when $d=0$. E_0 is the lowest hydrogenic level; E_e, the lowest even state when $d\neq0$.

singular near the impurity and the state cannot be localized at the impurity.

The splitting between the lowest even and odd states can be large. For values of ϵ, m_*, and d appropriate for $(CH)_x$, we solve Eq. (6) numerically. The lowest two eigenvalues for even states are -0.2229 and -0.0111 eV and for odd states are -0.0195 and -0.0049 eV. The energies of the odd states are very close to those (-0.0200 and -0.0050 eV) for the Coulomb problem. However, the lowest even impurity level is 0.223 eV below the band edge at 0.7 eV even though the "hydrogenic" level is very close to the edge. An energy of 0.44 eV is needed to form a charged kink on an undoped chain.[2] Thus the charged kink is only slightly more stable than the impurity state. A comparison using the results and parameters of Rice and Mele[8] leads to the same conclusion. In view of the simplicity of the SSH model and the dopant model, the difference in energy is not significant. Thus the effect of the impurity on the kink and polaron lattice distortions must be considered carefully.

A kink distortion of the lattice centered at x_k with a halfwidth l_k has the form

$$u_n=-(-1)^n u_0 \tanh\left[\frac{(x_n-x_k)}{(l_k a)}\right] . \tag{7}$$

The kink switches the phase of bond alternation at the center of the distortion. This distortion is an excited state of the chain with a midgap electronic state localized to the transition region. We distinguish two different kinks, strong and weak, which are useful for describing the results when kinks are centered at lattice sites. A strong (weak) kink has strong (weak) bonds on each side of the kink center (see Fig. 1).

A polaron distortion centered at x_p with halfwidth l_p and amplitude A_p has the form

$$u_n=(-1)^n u_0\left[1-A_p\exp\left[\frac{-(x_n-x_p)^2}{(l_p a)^2}\right]\right]. \tag{8}$$

The phase of bond alternation is the same on both sides of the polaron but differs by π for the kink. Moreover, the amplitude of bond alternation vanishes at the center of a kink but can be finite at the center of a polaron. Campbell and Bishop[10] obtained solutions for the polaron using the continuum limit of Eq. (1). Their form for u_n is the sum of two tanh's similar to Eq. (7). We have chosen the Gaussian form because it has only three variational parameters while Campbell's polaron has an additional parameter.

We find the electron eigenstates by numerical diagonalization of the tridiagonal matrix $H+U_{\rm imp}$ for chains with up to 700 sites. The energy of the system is found by summing the energies of the occupied states and finding the lattice energy in Eq. (1) for the appropriate distortion. End effects are eliminated by placing the distortion close to the impurity which is near the middle of the chain. When kinks are considered, an antikink is added at one end of the chain to further minimize end effects. We mimic the infinite chain of SSH by not allowing any relaxation of the bond alternation that would occur for a finite chain.[16] The energies of kinks and polarons on undoped (doped) chains are calculated relative to the ground-state energy of the neutral undoped (doped, but without the transferred electron) dimerized chain. A charged distortion on the doped chain is stable if the distortion has a lower energy than the dopant level of the doped dimerized chain. For fully screened dopants, the energies of kinks, polarons, and impurity states are insensitive to the length of the chain except for small differences ($\simeq$0.001 eV between 300 and 500 site chains) due to the long range of the Coulomb potential. When the Kivelson potential is used, the energies are more sensitive to chain length.

We use the parameters of SSH: $t_0=2.5$ eV, $t_1=2\alpha u_0=0.35$ eV, and $K=21$ eV/Å^2. We use the value[17] $\alpha=4.16$ eV/Å rather than 4.1 eV/Å of SSH because we get better agreement with the kink energies found by SSH using the first value. For the distance d between the impurity and the chain, we assume[2,8] that $d=2$ Å. We have also done calculations using $d=2.4$ Å. In the latter case, the potential is weaker. The impurity is slightly less important but the results are qualitatively the same. The values of d were chosen because they were used by SSH (Ref. 2) and because they are appropriate values for impurities sitting between chains.

All the calculations were performed for chains with an even number of sites. Chains with an odd number of sites have midgap states even when fully dimerized. When a simple lattice distortion is added, the number of midgap states changes by an even number. By considering only paired kink-antikink distortions, each kink or antikink has the appropriate odd number of gap states. All calculations for doped chains were performed with a single impurity present. When a kink-antikink distortion was considered, we could also have considered chains with two impurities to preserve the symmetry between kinks and antikinks. That procedure is unnecessary because the kink near an impurity is insensitive to an antikink located far from the impurity and the kink. Because we need not consider pairs of impurities, we truly model the effects of a single isolated dopant.

A proper inclusion of correlation is also a necessity, especially for the most attractive potentials that we consider. Correlation destabilizes the charged kink[8,17] and increases its width. Rice[8] estimated the correlation energy to be $U_c\simeq 2.65$ eV$/l_k$ for a charged kink. We use this estimate to evaluate the effect of correlation on our results. However, explicit calculations using the unrestricted Hartree-Fock scheme[17] would be more appropriate and would provide a more reliable estimate of the correlation. We have not attempted such calculations yet. They require a self-consistent determination of eigenfunctions, in addition to the eigenvalues, using more time consuming numerical procedures.

III. RESULTS

Our results for free kinks and polarons agree excellently with other calculations. For a pure $(CH)_x$ chain, the most stable kink has a halfwidth $l_k=7$ and an energy of 0.440 eV, almost exactly the results of SSH. The singly charged polaron on an undoped chain has an energy of 0.625 eV, a halfwidth $l_p=12$, an amplitude $A_p=0.6$, and gap states at $\pm$0.484 eV. These results are very close to those of Campbell[10] even though we use a different form for the u_n. The impurity states found by diagonalization of the Hamiltonian also agree surprisingly well with those determined with the effective-mass equation. Gap states occur 0.2216, 0.0230, and 0.0122 eV below the conduction-band edge for a fully screened dopant adjacent to a site (denoted FSS, $\epsilon=10$ at each site). This agreement confirms that the correct choice for the effective mass m_* is $0.146m_e$ rather than the value $m_*\simeq m_e$ used originally.[6,18]

The densities of states (DOS) for the dimerized chain (300 CH groups), the chain with a kink-antikink distortion, the chain with a polaron and the dimerized chain with a single FSS impurity are shown in Figs. 4 and 5. Even when the DOS of a dimerized lattice is plotted as a histogram, the square-root singularities at the band edges are obvious. When a kink-antikink or a polaron is added, states shift toward the gap. The changes in the DOS are similar in each case except near the gap. Two midgap states occur in the first case and a pair of states at ± 0.47 eV occur for the polaron. The square-root singularities remain for both. In contrast, the modification of the DOS is much greater when a dopant is added, even for the FSS dopant used for Fig. 5. States are shifted to lower energy by the attractive dopant potential. The band edge at -5.0 eV is broadened to energies below the band and the edge at 0.7 eV is broadened into the gap. The singularities at the other edges are also substantially broadened to lower energies. Obviously, the bands are not rigid, but can be modified greatly by an impurity.

Large shifts occur in the gap states of a kink-antikink pair when an impurity is present. We investigate these modifications by performing a series of calculations with an impurity near the center of a long chain, an antikink fixed at one end of the chain, and a kink on the chain but far from the antikink. The position of the kink is varied. When it is far from the impurity, states occur at the dopant levels of an impurity near a dimerized chain and at midgap for free kink-antikink states. If the kink is near the impurity, then the states localized to the kink and to the impurity can overlap. When they overlap the associated energy levels repel each other. The results for a fully screened dopant are shown first in Fig. 6 for a kink-antikink with $l_k=5$ (the most stable charged kink near the FSS dopant) and in Fig. 7 for $l_k=15$ (the most stable charged kink when the phenomenological correlation energy of Rice is included). In the first case the midgap state is pushed down to a quarter of the gap when the kink is pinned to the impurity. The lowest dopant level is pushed up by 0.13 eV. When $l_k=15$ two additional gap states appear. For a free kink ($l_k=15$), these extra states occur at ± 0.596 eV. These extra states are not as localized as the midgap states. Even when the dopant and kink are far apart, the dopant level overlaps the extra states and is repelled to lower energies by the state at 0.596 eV. At small n_k, the dopant level is pushed up by the

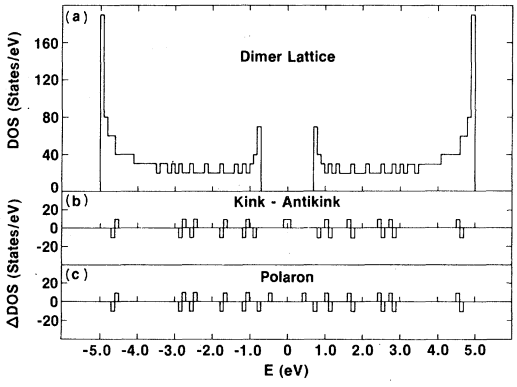

FIG. 4. Density of states of (a) a pure dimerized chain with 300 CH groups. Change in the density of states when (b) a kink-antikink distortion, $l_k=5$, or (c) a polaron, $l_p=8$ and $A_p=0.8$, is present.

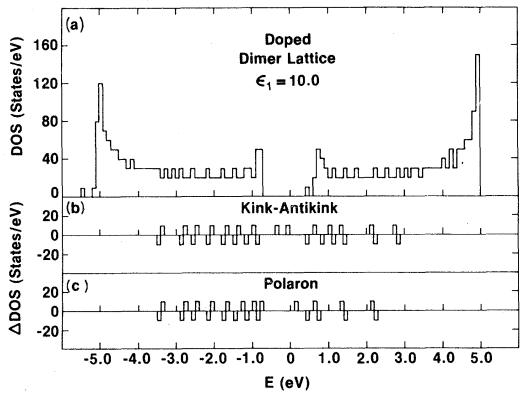

FIG. 5. Density of states of (a) a doped dimerized chain, one FSS impurity for 300 sites. Change in the density of states when (b) a kink-antikink, $l_k=5$, or (c) a polaron, $l_p=8$ and $A_p=0.8$, is pinned to the impurity.

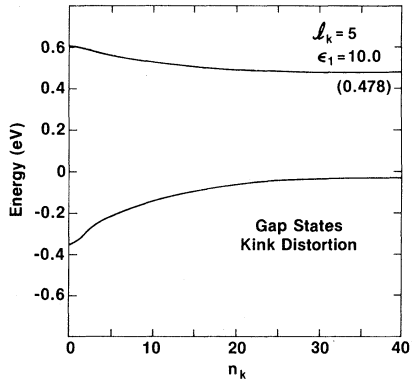

FIG. 6. Gap states of a doped chain with a kink-antikink distortion ($l_k=5$). Kink is centered n_k sites from the impurity. Dopant is an FSS impurity. Energy in parentheses is the value for large n_k. Only the lowest dopant level is shown. Antikink midgap state is not shown.

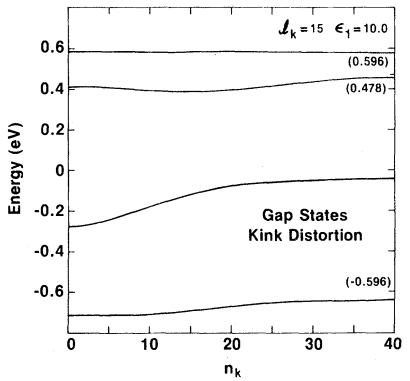

FIG. 7. Gap states of a doped chain with a kink-antikink distortion ($l_k=15$). FSS potential is considered. Only the lowest dopant level is shown. Antikink midgap state is not shown.

midgap state. As a result, the shifts of energy levels are much more complicated for large l_k.

The energy of charged kink formation on a doped chain depends on how the gap states are filled. When a neutral-kink—neutral-antikink pair occurs on an undoped chain, the midgap state of each is singly occupied, the two electrons coming from the valence state used to make the two midgap states. A kink is charged if two electrons occupy the midgap state. If the kink is near an impurity, the prescription for filling the states is not clear cut because the kink and antikink are no longer equivalent. The kink state is below midgap and is occupied by the two valence electrons, when the chain is neutral, forming a charged kink near the impurity and an oppositely charged antikink far from the impurity. When the charge donated by

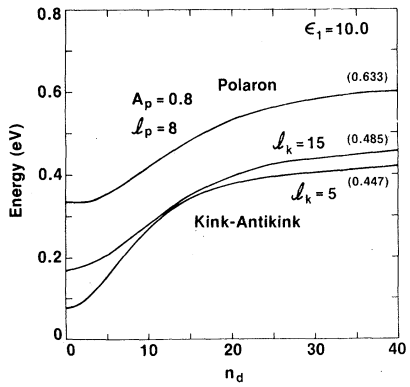

FIG. 8. Energy of charged kink and polaron distortions as a function of the separation n_d of the distortion from a FSS dopant. Parameters for the polaron and the kinks are shown. Values in parentheses give the free kink and polaron energies. Correlation is not included.

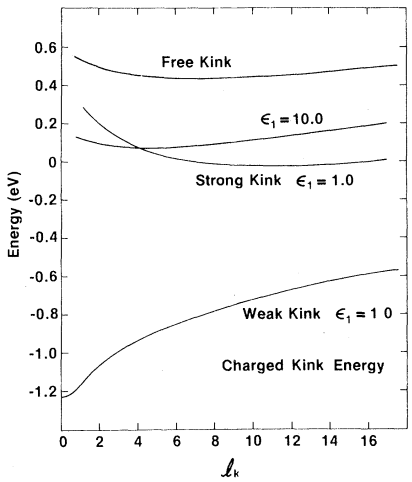

FIG. 9. Energy of charged kinks as a function of halfwidth l_k for a free kink, strong and weak kinks pinned to incompletely screened ($\epsilon_1=1.0, \Lambda=2.0$) dopants that are adjacent to sites, and strong and weak kinks pinned to FSS dopants. In the latter case, strong and weak kinks are nearly identical.

the impurity is added to the chain, it can occupy either the impurity state or the midgap state of the antikink. The first configuration is unstable because the impurity state is above midgap. Thus the midgap antikink state is occupied. The configuration of a charged pinned kink and a neutral antikink is not normally stable either if the energy needed to form each is included. Doping via kink formation is possible only if the energy of the neutral antikink is ignored.[1–3] We adopt this convention when discussing kink formation during doping.

Figures 8 and 9 show the energies for charged-kink formation as a function of the separation between the kink and an FSS impurity and as a function of l_k. The most stable charged kink is pinned to the impurity and has a halfwidth ($l_k=5$) that is smaller than that of a free kink ($l_k=7$). The kink pinned to an FSS impurity has an energy of 0.075 eV and is more stable than the configuration of a filled donor level on a dimerized chain by 0.403 eV. When the separation between the impurity and kink increases, the kink energy and width increase to the free-kink values. The energy of a charged kink with $l_k=15$ is also shown in Fig. 8. When the phenomenological correlation energy of Rice is added, this charged kink is the most stable pinned kink. When the U_c is added to the energies in Fig. 8, the stable charged kink has an energy of 0.36 eV. This is still more stable than the configuration with an occupied dopant level on a dimer chain, but by only 0.12 eV.

These results point out the necessity of an accurate treatment of the dopant and the correlation. In the SSH model, the charged kink pinned to an FSS dopant is stable. In this case the threshold for optical absorption is the energy difference between the kink gap state at -0.35 eV and the impurity state at 0.60 eV. This is greater than is allowed by the observed midgap absorption.[4,5] If correlation is added, the charged kink is less stable but $l_k = 15$. For these wider kinks, the energy difference between the kink gap state and the dopant level (see Fig. 7) is consistent with the optical threshold. Consequently, the explanation that midgap absorption results from kink formation during doping is only consistent with the experimental findings if correlation is added to the SSH model. Such a result must remain tentative until a better treatment of correlation is attempted. Nonetheless, the presence of a dopant, even the fully screened impurity (which has the weakest potential that might be a realistic model), substantially alters the original explanation[2,4] of midgap absorption by kink states.

In the remaining part of this section we will consider what effects other models of the dopant might have on kinks and then we will present results for polarons on a doped chain. Figure 9 compares the energy of a charged kink pinned to an FSS dopant with the energy of a kink pinned to an incompletely screened dopant which is adjacent to a site ($\epsilon_1 = 1.0$ and $\Lambda = 2.0$, denoted ISS). In the latter case, the potential is unscreened at the site adjacent to the impurity and only partially screened at the nearest-neighbor sites. The potential is fully screened at all other sites. When pinned to FSS dopants, weak kinks are more stable than the corresponding strong kinks by only 0.004 eV. However, if a potential with large local screening corrections is considered, the weak and strong kinks are very different. The stable strong kink is wide, $l_k \sim 12$, even when correlation is ignored; it is pinned and is only slightly more stable than a kink pinned to a FSS dopant. On the other hand, the stable weak kink is very narrow, $l_k \sim 0.1$, with an energy of -1.22 eV. For almost every value of l_k, the pinned kink is the most stable one. The depinned kink is more stable only for strong kinks with $l_k \lesssim 2$.

The dependence of the pinned-kink energies, widths, and gap states, and the dopant states on the local screening ϵ_1, is shown in Fig. 10. The difference between weak and strong kinks is noticeable for potentials which are nearly fully screened ($\epsilon_1 \sim 8$) and significant for $\epsilon_1 \lesssim 6$. For $\epsilon_1 \lesssim 6$ less energy is needed to occupy the dopant level on a

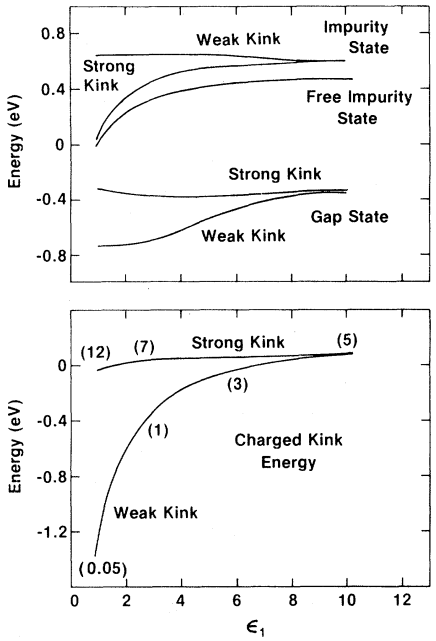

FIG. 10. Kink gap state, the lowest impurity level, and the energy of the stable charged kink pinned to a dopant which is adjacent to a site and incompletely screened ($\Lambda = 2.0$). Results for weak and strong kinks are shown. Lowest impurity level of a dopant on a dimer chain is also shown. Halfwidths for different ϵ_1 are shown in parentheses.

dimerized chain than to form a free charged kink. Thus the charged kink is stable when $\epsilon_1 \lesssim 6$ only if the interaction with the impurity is included. Furthermore, the optical threshold is above midgap for all ϵ_1 if a weak kink is present and for $\epsilon_1 \gtrsim 3$ if a strong kink is present. Consequently, the midgap absorption is not conclusive evidence for kink formation unless correlation really does suppress the level repulsion. The results were obtained for $\Lambda = 2.0$. For smaller Λ the incomplete screening is not restricted to the site adjacent to the impurity and to the nearest-neighbor sites and the effect of the dopant on the kink should be more pronounced.

To understand the difference between weak and strong kinks, we must consider the effect of the bond arrangement near the impurity. The weak pinned kink has long bonds on either side of the site adjacent to the impurity. The two regions of the lattice separated by the impurity couple only weakly through the pair of weak bonds. Thus the energy is minimized by lowering the energy of those occupied states which are localized to the dopant. This localization is enhanced if the kink is as abrupt as possible. The total energy is lowered even though there is little gain in lattice energy when the kink is

abrupt. The gap states are shown in Fig. 10. By increasing the localization of the gap levels, the repulsion between the empty donor level and the occupied kink state is enhanced. The former is pushed up nearly to the band edge and the latter pushed down to the valence edge. These shifts stabilize the kink. In contrast, the strong kink is much wider. With strong bonds on both sides of the impurity, extra charge is localized near the impurity. In this case, the energy is lowered by increasing the region where the lattice relaxes from the dimerized to the uniform configuration. This relaxation lowers the lattice energy. However, the band gap narrows during this relaxation and, as a consequence, the electronic energy should increase. This increase is compensated because the energy of the extra electrons localized to the uniform region is lowered by the dopant potential. Thus, the lattice can relax with little increase in electronic energy. Moreover the localized electrons are extended over a large region so the repulsion of the gap states is not important (see Fig. 10) as it is for weak kinks. When $\epsilon_1=1$ the donor state is at midgap and the kink state only 0.3 eV below the donor level.

These results for the weak kink may be too extreme to be realistic because correlation is not included and because the charge-transfer model may break down for such strong potentials. However, the results point out the dramatic changes that occur in the SSH model of kinks when other potentials are considered. These results also illustrate that the discrete nature of the $(CH)_x$ lattice is crucial if the dopant is incompletely screened. The continuum model for $(CH)_x$ would not predict a difference between weak and strong kinks.

So far we have discussed dopants which are adjacent to sites. There is little difference between the kinks pinned to FSS impurities and those pinned to fully screened impurities adjacent to midbonds. Moreover, in our phenomenological model an impurity near midbond is nearly fully screened at each site even when $\Lambda=2.0$. Thus the energy of a kink pinned to such an impurity is only 0.05 eV lower than that of a kink pinned to an FSS dopant.

One important difference does occur when the impurity is adjacent to the middle of a bond. In that case, a kink centered on one side of the impurity reverses the phase of the bond alternation at the impurity while a kink on the other side leaves the phase unchanged. The kink energy is lower if the kink weakens the bond. Consequently, kinks centered on one side of the impurity have lower energies than kinks on the other side. This difference is small in our model (0.002 eV if $\Lambda=2.0$) but would be much larger if the incomplete screening of impurities adjacent to midbonds were not minimized as it is by our model. In addition, the kink energies are lower by $0.01-0.02$ eV if the dopant is originally adjacent to a short bond in the dimer lattice because the kink weakens the bond.

If the dopant potential is modeled with anisotropic screening, the distortion of the kinks is even more drastic than if isotropic screening is used because the potential is screened by $\epsilon_\perp$ rather than $\epsilon_\parallel$ at large distances. For $(CH)_x$ $\epsilon_\parallel \sim 10$ while $\epsilon_\perp \sim 1-3$. The potential is so attractive at large distances that there are noticeable differences in the results for long and short chains. For example, when $\epsilon_\perp=1$ the midgap state of the antikink far from the impurity is 0.07 eV lower on the 300-unit chain than on a 700-unit chain. The perturbation caused by this potential is so large that on a doped dimer lattice one level originally in the conduction band is pulled into the valence band and (on a 700-unit chain) 20 states appear in the gap, including levels at -0.30, 0.04, and 0.25 eV. When $\epsilon_\perp=3$ there are 11 states in the gap including levels at 0.002, 0.46, and 0.59 eV. The distortion of pinned-kink gap states is also large. If $\epsilon_\perp=3$, the stable kink has a width $l_k \sim 4$, the gap state of the kink is pulled into the valence band and the lowest impurity state is pushed up to 0.25 eV. If $\epsilon_\perp=1$, then the kink gap state is also pulled below the valence-band edge. In addition, the lowest impurity level is below midgap. As a result, the midgap state of the antikink at the end of the chain loses its charge to the impurity level and the antikink is charged.

If anisotropic screening is the correct model for screening, then the SSH model for kink formation must be abandoned. Kink gap states are not the only states in the gap. Rather, the kink states are pulled out of the gap and the impurity states spread throughout the gap when anisotropic screening is used. Kink formation is meaningless because the distortions are so large. Proper inclusion of correlation into the SSH model may reduce this distortion but it is not clear that including correlation is enough.

The other distortion of $(CH)_x$ which has been considered extensively is the polaron. We now present our results for these distortions. We first consider a chain with an FSS dopant. The DOS of the stable pinned polaron is shown in Fig. 5. The DOS of the charged pinned polaron and charged kink-antikink pair on a doped chain are nearly identical, as they were for the free polaron and

kink-antikink. The only differences occur near midgap. As before, the changes are minor compared to the changes of the DOS caused by the dopant.

The calculations for polarons were performed as the calculations for kinks were done. The polaron was centered at different sites along the chain and the stable polarons found by varying A_p and l_p. When an FSS dopant is present, the stable charged polaron is pinned to the impurity, has an energy of 0.33 eV, an amplitude $A_p=0.8$, and a halfwidth $l_p=8$. This polaron is more stable than either a charged free kink or the filled dopant level on a dimer chain. Figure 8 shows the increase in polaron energy when the polaron is farther from the dopant. The results in Fig. 8 are for a polaron with $A_p=0.8$ and $l_p=8$. The most stable polaron at each separation $n_p\neq 0$ has a slightly lower energy than the polaron with $A_p=0.8$ and $l_p=8$; it also has a smaller amplitude ($A_p\rightarrow 0.6$ for large separations) and is wider ($l_p\rightarrow 12$ for large separations).

The dependence of the gap states on the separation between the polaron and an FSS dopant is shown in Fig. 11. Both polaron gap states are lower than the impurity state when the polaron and the impurity are widely separated. When the polaron approaches the impurity, both polaron states are repelled to lower energy by the impurity state. This repulsion helps stabilize the pinned polaron. Interestingly, the highest occupied state of the pinned polaron, at 0.18 eV, is only 0.47 below the empty dopant state. Thus the threshold for optical absorption is below midgap. Unlike the pinned charged kink, the charged polaron not only is more stable than the free kink and the filled dopant state on a dimerized chain but it also has a consistent optical threshold.

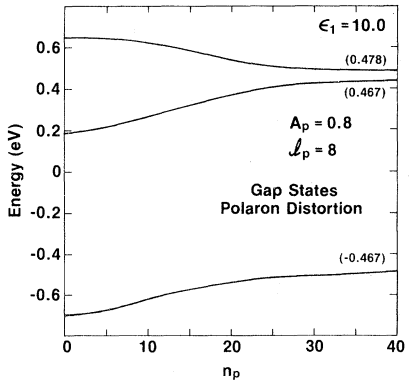

FIG. 11. Gap states of a doped chain with a polaron distortion ($A_p=0.8, l_p=8$). Dopant was modeled by a FSS dopant. Only the lowest dopant level is shown. Polaron center is n_p sites from the impurity. Energies in parentheses are for a widely separated polaron and impurity.

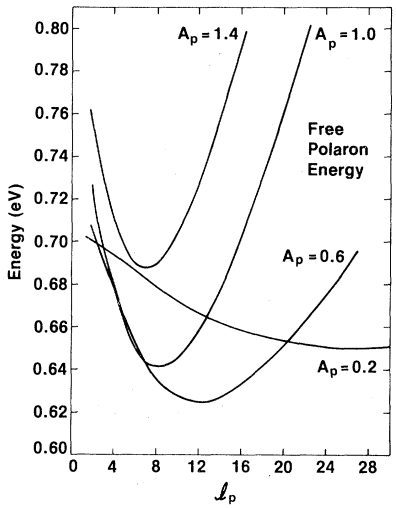

FIG. 12. Energies of polarons on an undoped chain as a function of halfwidth l_p and amplitude A_p.

The dependence of a free charged polaron's energy on A_p and l_p is shown in Fig. 12. The dependence on A_p and l_p is similar for polarons near impurities. For a fixed A_p, the polaron energy is approximately a quadratic function of l_p. The width of the most stable polaron with a given A_p varies approximately as the inverse of A_p. Moreover, the stable polaron energy depends roughly quadratically on A_p with a minimum at $A_p=0.6$. This quadratic behavior is valid only near this minimum. The effective spring constant of the polaron potential energy is much weaker at large A_p and l_p than at

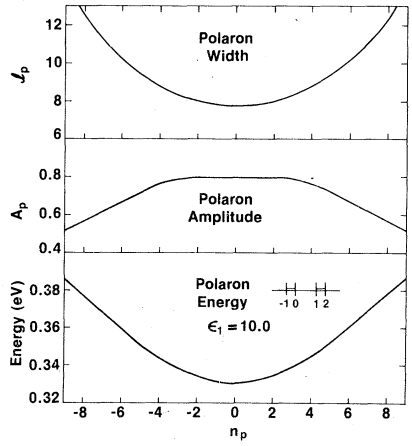

FIG. 13. Polaron halfwidth, amplitude, and energy for the most stable polaron centered at site n_p with a FSS dopant at site 0. Bond pattern used for the dimer lattice is shown.

small A_p and l_p.

The results for depinned polarons near an FSS dopant are similar. The width, amplitude, and energy of the most stable polaron centered at a given site n_p relative to an FSS dopant that is adjacent to site 0 are shown in Fig. 13. The lattice configuration of the dimer lattice is also shown in the figure. When $|n_p| \gtrsim 8$, the charged polaron actually is wider and has a smaller amplitude than the free polaron. The polaron is free only for much larger $|n_p|$. This discrepancy occurs because for $|n_p| \sim l_p$ the polaron energy can be lowered if the polaron and its gap states are wide enough to overlap the impurity state and benefit from the repulsion with that state.

When a fully screened impurity is adjacent to a site the polaron energy is not a symmetric function of n_p, although the differences are not apparent in Fig. 13. For the lattice configuration assumed in the figure, polarons centered at negative n_p have a lower energy (by ~ 0.001 eV) than those at the corresponding positive n_p. This occurs because the polaron at negative n_p increases the average bond length near the impurity (the distance between sites -1 and 1 in the figure) while the polaron at positive n_p reduces this distance. As with kinks, weakening the local bonds lowers the polaron energy. The energies do not change much if the fully screened dopant is adjacent to the middle of a bond. However, because of the symmetry of the impurity location, the small difference between polarons on different sides of the dopant vanishes.

In view of the simplicity of the SSH model and the dopant model, the magnitudes of these small differences have no significance. However, they do point out the trends that occur for dopants modeled with incomplete screening. For the extreme case of an ISS dopant, the charged-polaron energies are negative (see Fig. 14). Moreover, those centered at negative n_p are very different from those at positive n_p. The difference is signaled by the sharp transition in behavior at $n_p \sim 0$. Those polarons at negative n_p increase the average bond length near the impurity and have much lower energies. For $n_p < 0$ the amplitude $A_p \gtrsim 2$ so that the bond alternation is actually reversed at the center of the polaron. Because $l_p \sim |n_p|$, the increase in average bond length is a maximum near the impurity. For $n_p \sim -1$, the polaron is very narrow, just as the weak kink is. The most stable polaron is not pinned but rather is at $n_p \sim -1.5$. For $n_p > 0$, the charged polaron is similar to the free polaron with $A_p < 1$ and $l_p \sim 10-20$.

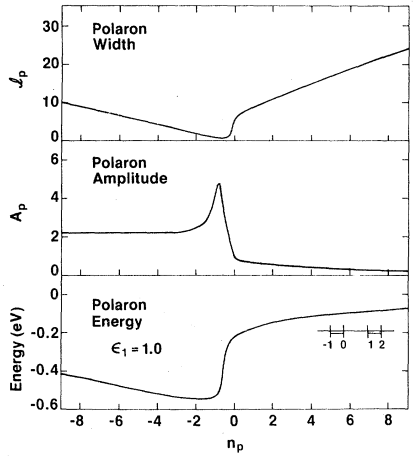

FIG. 14. Polaron halfwidth, amplitude, and energy for the most stable polaron centered at site n_p for a dopant at site 0 with incomplete screening ($\epsilon_1 = 1.0$ and $\Lambda = 2.0$). Bond pattern of the dimer lattice is shown.

IV. CONCLUSIONS

We have determined the effect that a dopant can have on the electron states and distortions of lightly doped polyacetylene by considering several models for the dopant potential. These models include dopants isotropically screened in two extreme fashions—with a bulk dielectric at each site and with no local screening. In addition, we have tested dopants screened anisotropically to phenomenologically account for the anisotropy of $(CH)_x$.

We find that the dopant potential can affect the band structure of $(CH)_x$, distort the kink states, and introduce impurity states away from the band edges. Even the fully screened dopant can introduce these modifications. When these changes are included, the charged kink near a fully screened dopant remains more stable than the configuration with no distortions. However, the predicted optical-absorption threshold is too high. On the other hand, the charged polaron is also more stable than the undistorted configuration (and more stable than the charged-kink—free-antikink pair, but not the charged kink alone) and the predicted optical threshold is consistent with the experimental observations. This suggests that the charged polaron may be the distortion formed during doping. However, the charged polaron has one unpaired spin and would not be consistent with the susceptibility measurements of Weinberger *et al.*[19] This objection can be removed but only if banding of the polaron states weakens the predicted Curie-type susceptibility[7] or if the experiments are incomplete or can be reinterpreted.[20]

Our results are very sensitive to the form of the dopant potential. When local screening corrections are included, the discrete nature of the $(CH)_x$ lattice is important. Kinks and polarons which weaken the bonds near the impurity are more stable than distortions which strengthen the bonds. Isotropically screened dopants introduce a few impurity levels into the gap. An anisotropically screened dopant pulls many levels into the gap. However, one result is common to all dopant models. The simple picture for doped $(CH)_x$ of rigid bands unaffected by the dopant is invalid for each of the dopant models considered.

Because of the sensitivity of the results to the model used, the nature of dopant states, kinks, and polarons in $(CH)_x$ cannot be reliably determined with simple models. Fundamental studies must be done to develop realistic models for the dopant, the screening and the electron-dopant interaction. Electron correlation must also be included in the SSH model, especially when potentials with incomplete or anisotropic screening are considered. We will report results for such extentions of this work in future publications. Until a realistic model of the dopant effects has been developed, the nature of doping in $(CH)_x$ must remain unclear.

ACKNOWLEDGMENTS

The assistance of R. Boisvert of the National Bureau of Standards in providing programs to perform the matrix diagonalization was invaluable. One of us (G.W.B.) gratefully appreciates support by a National Research Council—National Bureau of Standards fellowship. One of us (A.J.G.) thanks the United States—Israel Educational Foundation for a grant.

*Permanent address.

[1]W. P. Su, J. R. Schrieffer, and A. J. Heeger, Phys. Rev. Lett. 42, 1698 (1979).

[2]W. P. Su, J. R. Schrieffer, and A. J. Heeger, Phys. Rev. B 22, 2099 (1980).

[3]M. J. Rice, Phys. Lett. 71A, 152 (1979).

[4]N. Suzuki, M. Ozaki, S. Etemad, A. J. Heeger, and A. G. MacDiarmid, Phys. Rev. Lett. 45, 1209 (1980).

[5]H. Kiess, W. Meyer, D. Baeriswyl, and G. Harbeke, J. Electron. Mater. 9, 763 (1980).

[6]C. R. Fincher, Jr., M. Ozaki, A. J. Heeger, and A. G. MacDiarmid, Phys. Rev. B 19, 4140 (1979).

[7]G. W. Bryant and A. J. Glick, J. Phys. C 15, L391 (1982).

[8]M. J. Rice and E. J. Mele, Solid State Commun. 35, 487 (1980).

[9]F. E. Karasz, J. A. Hirsch, Y. Yamashita, and J. C. W. Chien, Bull. Am. Phys. Soc. 37, 167 (1982).

[10]D. K. Campbell and A. R. Bishop, Phys. Rev. B 24, 4859 (1981).

[11]H. Takayama, Y. R. Lin-Liu, and K. Maki, Phys. Rev. B 21, 2388 (1980).

[12]E. J. Mele and M. J. Rice, Phys. Rev. B 23, 5397 (1980).

[13]We could consider potentials modified by Thomas-Fermi screening by multiplying the potential in Eq. (3) by $\exp(-\Lambda_{TF}|x_n - x_{imp}|)$ where Λ_{TF} is the inverse screening length. However, Thomas-Fermi screening should be unimportant in lightly doped (semiconducting) $(CH)_x$. Such screening should be important only at doping densities of $\gtrsim 5\%$ when $(CH)_x$ is metallic.

[14]R. Loudon, Am. J. Phys. 27, 649 (1959).

[15]M. Andrews, Am. J. Phys. 44, 1064 (1976).

[16]W. P. Su, Solid State Commun. 35, 899 (1980).

[17]K. R. Subbaswamy and M. Grabowski, Phys. Rev. B 24, 2168 (1981).

[18]C. K. Chiang, C. R. Fincher, Jr., Y. W. Park, A. J. Heeger, H. Shirakawa, E. J. Louis, S. C. Gau, and A. G. MacDiarmid, Phys. Rev. Lett. 39, 1098 (1977).

[19]B. R. Weinberger, J. Kaufer, A. J. Heeger, A. Pron, and A. G. MacDiarmid, Phys. Rev. B 20, 223 (1979).

[20]Y. Tomkiewicz, T. D. Schultz, H. B. Bron, A. R. Taranko, T. C. Clarke, and G. B. Street, Phys. Rev. B 24, 4348 (1981).